www.impactjournals.com/oncotarget/ Oncotarget, 2017, Vol. 8, (No. 9), pp: 15520-15538

Research Paper

The nitrobenzoxadiazole derivative MC3181 blocks melanoma invasion and metastasis

Anastasia De Luca[1,*], Debora Carpanese[2,*], Maria Cristina Rapanotti[3], Tara Mayte Suarez Viguria[3], Maria Antonietta Forgione[4], Dante Rotili[4], Chiara Fulci[1], Egidio Iorio[5], Luigi Quintieri[6], Sergio Chimenti[7], Luca Bianchi[7], Antonio Rosato[2,8], Anna Maria Caccuri[1]

[1]Department of Experimental Medicine and Surgery, University of Tor Vergata, 00133 Rome, Italy

[2]Department of Surgery, Oncology and Gastroenterology, University of Padova, 35128 Padova, Italy

[3]Department of Laboratory Medicine, University of Tor Vergata, 00133 Rome, Italy

[4]Department of Drug Chemistry and Technologies, "Sapienza" University, 00185 Rome, Italy

[5]Department of Cell Biology and Neurosciences, Istituto Superiore di Sanità, 00161 Rome, Italy

[6]Department of Pharmaceutical and Pharmacological Sciences, University of Padova, 35131 Padova, Italy

[7]Department of Dermatology, University of Tor Vergata, 00133 Rome, Italy

[8]Istituto Oncologico Veneto IOV-IRCCS, 35128 Padova, Italy

[*]These authors have contributed equally to this work

Correspondence to: *Anna Maria Caccuri,* ***email:*** *caccuri@uniroma2.it*
Antonio Rosato, ***email:*** *antonio.rosato@unipd.it*

Keywords: *melanoma, 6-((7-nitrobenzo[c][1,2,5]oxadiazoles, c-Jun N-terminal kinase, antimetastatic properties, glutathione transferase P1-1*

Received: *July 25, 2016* ***Accepted:*** *December 27, 2016* ***Published:*** *January 17, 2017*

ABSTRACT

The novel nitrobenzoxadiazole (NBD) derivative MC3181 is endowed with remarkable therapeutic activity in mice bearing both sensitive and vemurafenib-resistant human melanoma xenografts. Here, we report that subtoxic concentrations of this compound significantly reduced invasiveness of BRAF-V600D mutated WM115 and WM266.4 melanoma cell lines derived from the primary lesion and related skin metastasis of the same patient, respectively. The strong antimetastatic activity of MC3181 was observed in both 2D monolayer cultures and 3D multicellular tumor spheroids, and confirmed *in vivo* by the significant decrease in the number of B16-F10 melanoma lung metastases in drug-treated mice. Our data also show that MC3181 affects the lactate production in the high glycolytic WM266.4 cell line. To unveil the MC3181 mechanism of action, we analyzed the ability of MC3181 to affect the degree of activation of different MAPK pathways, as well as the expression/activity levels of several proteins involved in angiogenesis, invasion, and survival (i.e. AP2, MCAM/MUC18, N-cadherin, VEGF and MMP-2). Our data disclosed both a decrease of the phospho-active form of JNK and an increased expression of the transcription factor AP2, events that occur in the very early phase of drug treatment and may be responsible of the antimetastatic effects of MC3181.

INTRODUCTION

Malignant melanoma progresses through a multi-step process switching from dysplasia to radial growth phase, to invasive vertical growth phase, and subsequently to distant metastases. These switches implicate the breach of the basement membrane by neoplastic proliferating cells, their migration and stroma invasion to enter the vasculature, and finally their extravasation and adhesion in distant organs to form a secondary tumor [1–3]. Every phase of this complex scenario can be rate-limiting and offers potential target for therapy.

Therapeutically, one of the most recent and promising approaches is immunotherapy that involves the use of immune checkpoint inhibitors enabling the interruption of T-cell pathways responsible for immune down-regulation or tolerance, such as the anti-CTLA-4 monoclonal antibody (mAb) ipilimumab, along with the anti-PD-1 mAbs pembrolizumab and nivolumab. Another important class of drugs is represented by low molecular weight compounds interfering with signaling pathways involved in the dysregulation of cell growth and proliferation; this is the case of vemurafenib and dabrafenib, which target mutated v-raf murine sarcoma viral oncogene homolog B1 (BRAF), the selective inhibitors of extracellular signal-regulated kinase (ERK), as well as trametinib and cobimetinib targeting mitogen-activated protein kinase (MAPK)/ERK Kinase (MEK) proteins [4]. While these strategies provide a potential initial clinical benefit, they delay but not prevent patient mortality due to the ability of tumor to rapidly acquire resistance to drugs and/or to activate alternative proliferation pathways.

In contrast with current clinical trials targeting multiple signaling pathways involved in cell proliferation, we recently reported that the nitrobenzoxadiazole derivatives (NBDs) NBDHEX [6-((7-nitrobenzo[c][1,2,5]oxadiazol-4-yl)thio)hexan-1-ol] and its more water-soluble analogue, MC3181 [2-(2-(2-((7-nitrobenzo[c][1,2,5]oxadiazol-4-yl)thio)ethoxy)ethoxy)ethanol], exert a potent antitumor activity through the activation of different MAPK pathways. These compounds represent a new class of antitumor agents exhibiting an outstanding therapeutic activity together with an extremely non-toxic profile in human cutaneous melanoma mouse xenografts. NBDHEX and MC3181 inhibit glutathione transferase P1-1 (GSTP1-1), and disrupt the GSTP1-1/JNK1 and GSTP1-1/TRAF2 complexes, thereby causing prolonged tumor cell cycle arrest and apoptosis. Therefore, these drugs may constitute a new effective strategy for the treatment of BRAF-mutated human melanomas, capable of overcoming the resistance to vemurafenib [5, 6].

On this ground, we were prompted to test the antimetastatic properties of the more soluble NBD derivative, MC3181, against melanoma cells lines derived from the primary lesion (WM115) and a skin metastasis (WM266.4) of a single patient harboring a BRAF-V600D mutation.

Our data revealed that subcytotoxic doses of MC3181 exert a strong antimetastatic activity *in vitro*. To understand the mechanism(s) underling this effect, we measured the expression/activity levels of key proteins involved in melanoma cells migration and invasion, and focused on signaling pathways that modulate these proteins. Moreover, using the B16-F10 melanoma mouse model of metastasis, we demonstrated that the oral administration of MC3181 exerts a potent antimetastatic effect, significantly suppressing and/or delaying lung metastasis in the absence of detectable sign of toxicity. These data provide evidence to further support the potential of MC3181 as a novel therapeutic to treat metastatic melanoma.

RESULTS

Antiproliferative activity of MC3181 and NBDHEX on WM115 and WM266.4 2D monolayer cultures and 3D multicellular tumor spheroids

The antitumor efficacy of MC3181 was tested *in vitro* on 2D WM115 and WM266.4 human melanoma cell cultures, and compared with NBDHEX, temozolomide (TMZ) and vemurafenib (VMF). The concentration–response profiles (Supplementary Figure 1) fulfill the IC_{50} values reported in Table 1. Of note, the IC_{50} values calculated for MC3181 are in the low micromolar range (1.0–1.3 μM), and close to those obtained for both NBDHEX and vemurafenib (VMF), whereas TMZ is at least 600 times less effective.

Next, we decided to evaluate the effect of MC3181 and its parent drug, NBDHEX, on 3D multicellular tumor spheroids, which are more precise in mimicking the complex organization of tumor tissue *in vivo* [7]. Spheroids were treated with graded concentrations of MC3181 (Figure 1b and 1d) or NBDHEX (Figure 1c and 1e), and IC_{50} values were obtained by analyzing both cell viability (MTS) and growth rate. A schematic diagram for treatment schedule and analysis (cell imaging and viability assay) is shown in Figure 1a. We noticed that WM266.4 spheroids grew faster increasing their volume 25 times at the end of the experiment (day 17, Figure 1d and 1e), whilst the WM115 counterparts augmented only 8 times (Figure 1b and 1c). The IC_{50} values of MC3181 on WM266.4 spheroids were in the low micromolar range (0.5–7.7 μM, Table 2), comparable at both 48 hours and 17 days, and similar to those obtained with NBDHEX. In contrast, 48 hours treatment with both MC3181 and NBDHEX caused flaking of WM115 spheroids and formation of poorly defined contours that did not allow an accurate measurement of spheroids' diameter (data not shown). Additionally, after 17 days of treatment, the spheroids' viability dropped more slowly compared to the spheroids' volume, resulting in loss of linear relationship between viability and cell number (Table 2). A similar event has been already reported and explained by the occurrence of cell cycle arrest [8].

Effect of low concentrations of MC3181 on cell proliferation and cell cycle

Since MC3181 and NBDHEX showed comparable activity in both WM115 and WM266.4 cells, we focused on the antimetastatic efficacy of the more water soluble

Table 1: Evaluation of the antiproliferative (SRB assay) effects of MC3181, NBDHEX, VMF and TMZ on WM115 and WM266.4 2D monolayer cultures

Cell line	IC_{50} ± SD (μM)			
	MC3181	NBDHEX	VMF	TMZ
WM115	1.28 ± 0.02	1.99 ± 0.01	2.47 ± 0.19	1196 ± 103
WM266.4	1.07 ± 0.04	0.94 ± 0.04	0.89 ± 0.01	800 ± 5

NBD derivative, namely MC3181. We investigated three different concentrations of MC3181 for each cell line: WM115 and WM266.4 cells were treated with MC3181 concentrations of 1.3 and 1.0 μM respectively (corresponding to their IC_{50} values), 0.26 and 0.20 μM respectively (corresponding to 1/5 of their IC_{50} values) and 0.05 and 0.04 μM respectively (corresponding to 1/25 of their IC_{50} values).

We analyzed cell proliferation and cell cycle at different time points after the addition of MC3181. A decrease in the WM115 growth rate was observed after 24 hours incubation with both 0.26 and 1.3 μM MC3181 (Supplementary Figure 2a), which corresponds to a significant arrest in the G2/M phase of the cell cycle (Supplementary Figure 2b). In contrast, WM266.4 showed only a slight decrease of cell proliferation after 48 hours treatment with the highest MC3181 dose (1.0 μM) (Supplementary Figure 2c). In accordance, the WM266.4 cell cycle was only slightly affected by treatment with 1.0 μM MC3181 (Supplementary Figure 2d).

MC3181 treatment affects the adhesion properties of both WM115 and WM266.4 cells

The successful dissemination of tumor cells and the formation of new tumor foci require cancer cells adhesion and detachment from components of the extracellular matrix (ECM) and basement membrane (BM). Therefore, we analyzed the effect of MC3181 on the adhesion properties of WM115 and WM266.4 cells to different ECM components, i.e. type I collagen, Matrigel and gelatin [9, 10].

The primary tumor-derived WM115 cells showed poor basal adhesion on both gelatin and Matrigel (Figure 2b and 2c). The treatment with 0.26-1.3 μM MC3181 reduced to approximately 50% their adhesion to collagen (Figure 2a), whilst a concentration-dependent effect was observed on gelatin (Figure 2b), reaching an adhesion inhibition of 84% at 1.3 μM MC3181. This drug concentration was also able to abolish (96%) the adhesion of WM115 on Matrigel (Figure 2c).

The skin metastasis-derived WM266.4 cells showed excellent adhesion properties on all the substrates tested (Figure 2d-2f). However, the sensitivity to MC3181 was clearly lower than that of WM115. Indeed, 0.04 μM MC3181 was sufficient to induce 40% reduction of cell adhesion to collagen (Figure 2d), but a significant effect (80% inhibition) on gelatin adhesion was evident only with 1.0 μM MC3181 (Figure 2e). Finally, MC3181 did not show any significant inhibitory effect on tumor cell adhesion to Matrigel (Figure 2f).

MC3181 inhibits invasion of human melanoma cells *in vitro*

Another aspect of tumor progression is the ability of tumor cells to invade basement membranes and connective tissue leading to the possible formation of distant metastases. We investigated the migratory and invasive potential of both primary tumor (WM115) and metastasis-derived (WM266.4) melanoma cells after 48 hours treatment with MC3181. This compound efficiently suppressed invasion in both cell lines, without any effect on their migration (Figure 3a, 3b, 3f and 3g). Of note, a concentration of MC3181 corresponding to 1/25 of its IC_{50} value (0.04 μM) was capable of inducing 75% reduction of WM266.4 invasion index (Figure 3h), while an equiactive concentration of MC3181 (0.05 μM) reduced the invasion index of WM115 by approximately 30% (Figure 3c). However, 60% inhibition of WM115 invasion index was obtained with 0.26 and 1.3 μM. Further, we evaluated the antimetastatic properties of MC3181 in a third tumor cell line, namely the BRAF-V600E-mutated SK-MEL-5 human melanoma cell line, which has been established from an axillary lymph node metastasis. Based on the finding that in the SRB assay MC3181 exhibited an IC_{50} value of 1.6 ± 0.1 μM towards SK-MEL-5 cells (data not shown), invasion/migration assays were carried out using the following drug concentrations: 1.60 μM (i.e., the IC_{50}); 0.32 μM (i.e., 1/5 of IC_{50}); and 0.06 μM (i.e., 1/25 of the IC_{50}) (Supplementary Figure 3). The invasive potential of SK-MEL-5 cells was reduced by approximately 30% by 0.32 μM MC3181 whereas, a 60% inhibition was recorded at a drug concentration of 1.6 μM. Furthermore, MC3181 significantly depressed migration of SK-MEL-5 cells (Supplementary Figure 3a and 3b). Of note, a 50% reduction of cell migration was achieved with 0.32 and 1.6 μM MC3181. Since the drug inhibited both SK-MEL-5 cell invasion and migration, no change of the invasion index occurred (Supplementary Figure 3c).

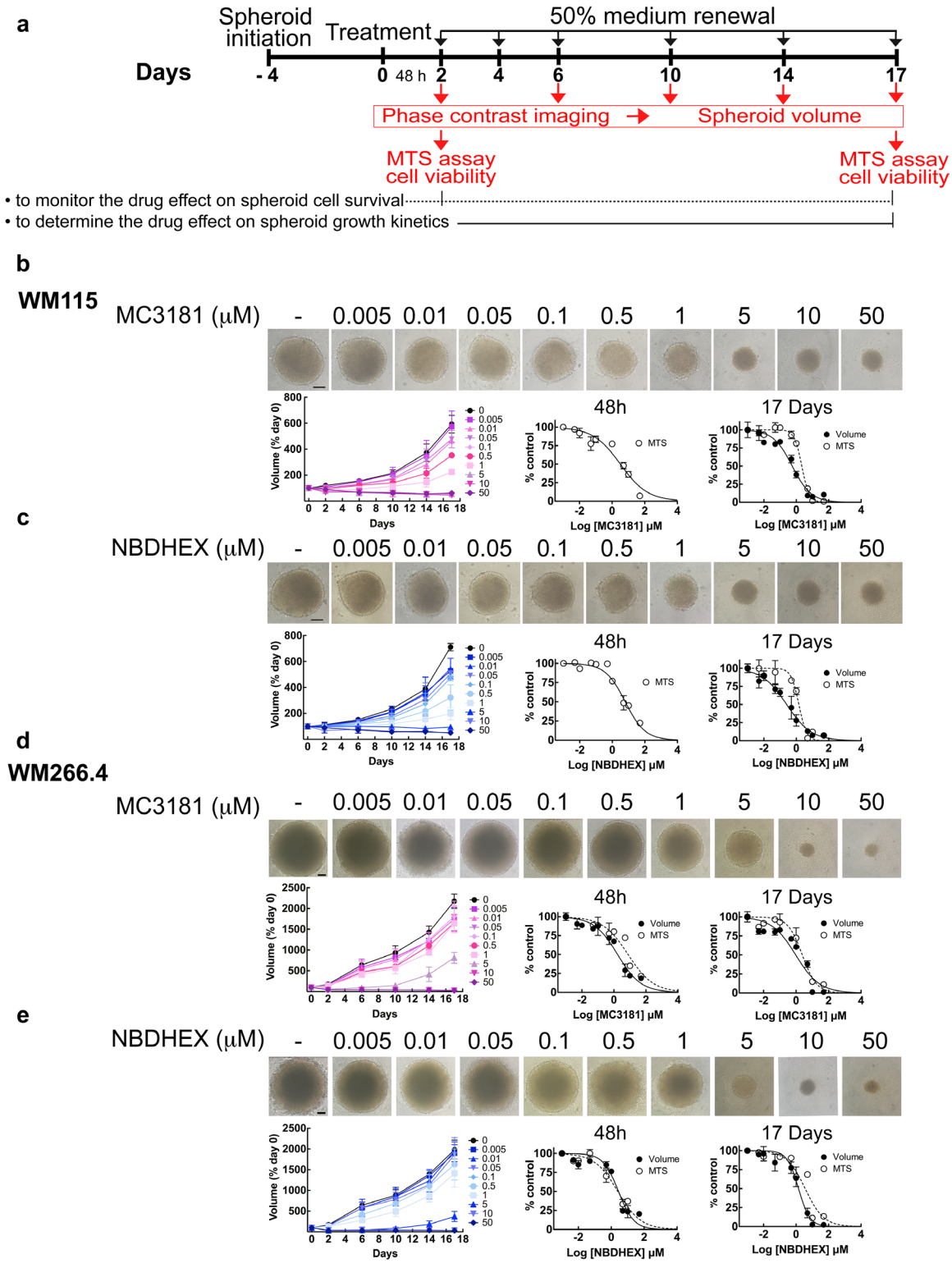

Figure 1: MC3181 and NBDHEX concentration-dependent inhibition of tumor spheroid growth. a. Schematic illustration of tumor spheroid growth kinetics and compound treatment procedures. Spheroids were treated with drug or drug vehicle 4 days after cell plating (day 0); 50% medium replenishment was performed on days 2, 4, 6, 10 and 14. **b-c.** WM115 and **d-e.** WM266.4 spheroids treated with graded concentrations of MC3181 (b and d) or NBDHEX (c and e). Control spheroids were treated with vehicle. Spheroid growth kinetics (left) was evaluated by phase contrast imaging at day 2, 6, 10, 14 and 17, whereas the concentration-response curves relative to the MTS assays and spheroid volume analysis were obtained after 48 hours (center) and 17 days (right) of drug treatment. Phase contrast images (10X magnification, 3X digital magnification) correspond to 17 days treated spheroids. Scale bar: 100 μm. Values are means ± SD (n = 12).

Table 2: Evaluation of the cytotoxic (MTS assay) and antiproliferative (volume analysis) effects of MC3181 and NBDHEX on WM115 and WM266.4 3D multicellular tumor spheroids

	IC_{50} ± SD (μM)			
	WM115			
	48 hours		17 Days	
	Volume	MTS	Volume	MTS
MC3181	n.d.	3.22 ± 0.19	0.53 ± 0.04	2.19 ± 0.15
NBDHEX	n.d.	1.44 ± 0.08	0.37 ± 0.09	6.27 ± 0.94
	WM266.4			
	48 hours		17 Days	
	Volume	MTS	Volume	MTS
MC3181	1.67 ± 0.26	7.67 ± 1.00	1.10 ± 0.23	2.41 ± 0.40
NBDHEX	2.84 ± 0.19	2.44 ± 0.43	1.22 ± 0.33	3.60 ± 0.51

MC3181 treatment reduces MMP-2 intracellular activity

We next examined MMP-2 activity in WM115 and WM266.4 melanoma cells by gelatin zymography (Figure 3d, 3e, 3i and 3l). Densitometric analysis showed that treatment of both cell lines with equiactive concentrations of MC3181 induced a reduction of the MMP-2 activity in a concentration-dependent manner. In particular, a significant inhibition of MMP-2 proteolytic activity was observed in WM115 and WM266.4 cells treated with a concentration of MC3181 corresponding to the IC_{50} value in these cell lines (i.e., 1.3 and 1.0 μM, respectively) (Figure 3e and 3l).

MC3181 affects invadopodia formation in WM115 and WM266.4 melanoma cell lines

The strong effect of MC3181 prompted us to investigate the possible effect of the drug on the formation of invadopodia, protrusions emanating from the surface of cells and characterized by a high proteolitic activity towards the ECM. We examined the ability of WM115 and WM266.4 cells to degrade fluorescein-gelatin by observing the loss of fluorescence of the labeled gelatin and its correspondence with phalloidin structure, which identifies invadopodia puncta (Figure 4a and 4d). In addition, the presence of invadopodia was confirmed by measuring the fluorescence intensity of TRITC-phalloidin (red line) and fluorescein-gelatin (green line) along an arbitrary line that crossed through neighboring invadopodia structures. Figures 4b for WM115 and 4e for WM266.4 show a drastic decrease of the green fluorescence intensity in correspondence with an increase in the red fluorescence intensity of TRITC-phalloidin. Confocal microscopy analysis revealed a significant decrease in the number of cells with active invadopodia following treatment with concentrations of MC3181 corresponding to 1/5 and 1/25 of its IC_{50} value in these cell lines (Figure 4c and 4f). Moreover, the highest MC3181 concentrations (i.e., 1.3 and 1.0 μM for WM115 and WM266.4, respectively) completely inhibited adhesion of the cells to the fluorescein-gelatin layer. Under these conditions, it was not possible to estimate the percentage of cells with active invadopodia.

Effects of MC3181 treatment on intracellular metabolome of WM115 and WM266.4 melanoma cells

A comprehensive analysis of the effects of intracellular metabolome was carried out by quantitative ^{1}H-NMR spectroscopy on WM115 and WM266.4 cells following MC3181 treatment for 48 hours.

As shown in Supplementary Figure 4, we found a progressive decrease in the intracellular levels of lactate in the high glycolytic WM266.4 cells, while we did not found other metabolic changes in the same cells (see Supplementary Tables 1A and 1B). No evident effects on metabolome were found in WM115 cells treated at both low and high concentrations of MC3181.

Analysis of the effect of MC3181 treatment on the mRNA expression of a panel of genes involved in melanoma progression and metastatization

Qualitative RT-PCR was carried out to characterize WM115 and WM266.4 cell lines for the expression of a panel of genes, including the pro-angiogenic factors vascular endothelial growth factor (VEGF) and the basic fibroblast growth factor (FGF2); the matrix-metallo-

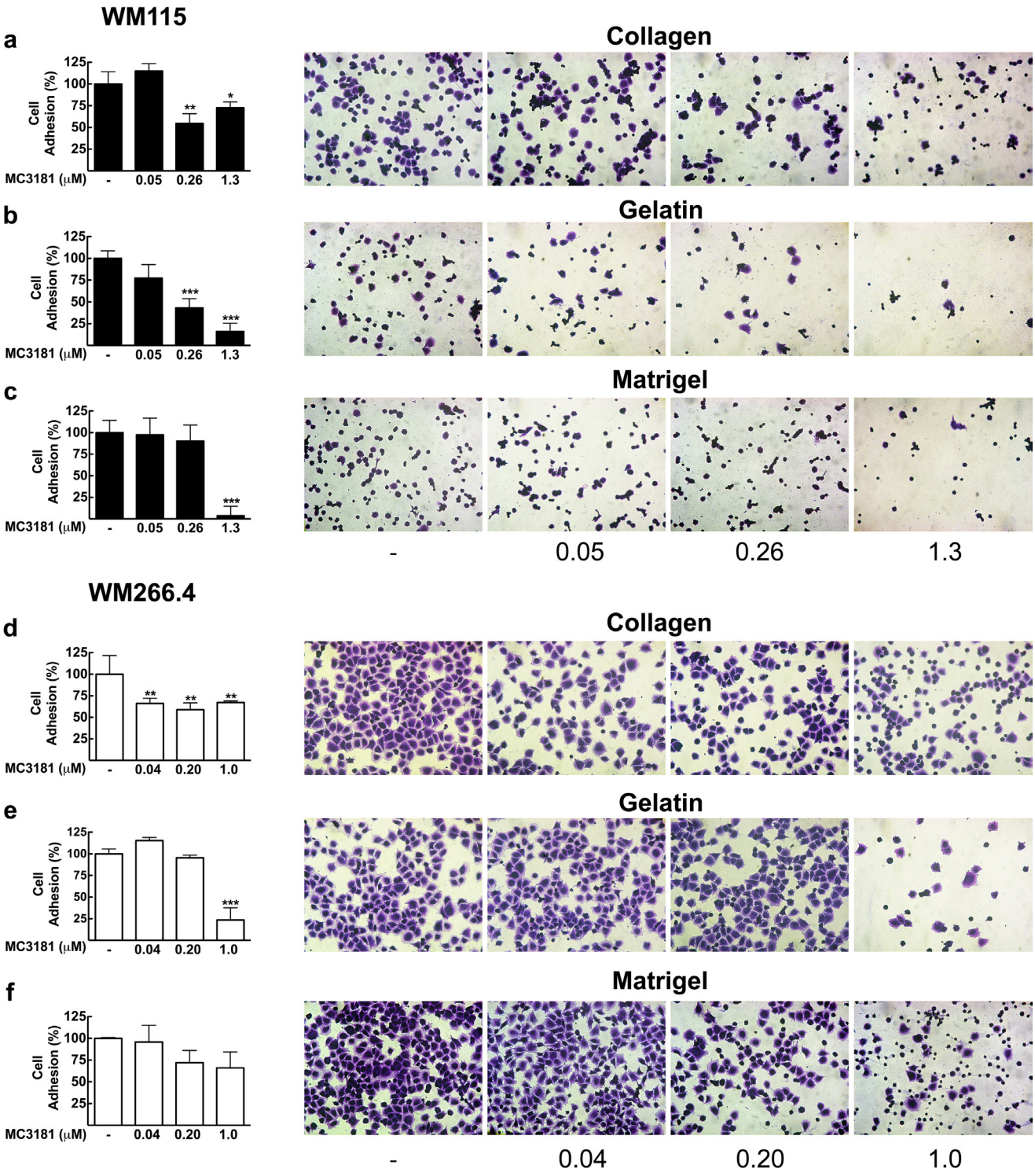

Figure 2: Effect of MC3181 on the adhesion of human melanoma cells to different ECM components. WM115 cells and WM266.4 cells ($3x10^5$/ml) were applied to individual coated wells with 200 µl of **a, d.** collagen (7.5 µg/ml), **b, e.** gelatin (0.1%) or **c, f.** Matrigel (0.2 mg/ml), in the absence and in the presence of increasing MC3181 concentrations, and incubated for 30 minutes at 37°C in 5% CO_2. Cells were then fixed and colored with crystal violet. Images (20X magnification, 3X digital magnification) were obtained by phase contrast microscopy. The absorbance values of wells were measured at 580 nm after dissolving crystal violet with 100% methanol. The results were expressed as the mean percentage of cell adhesion ± SD versus control, repeated in triplicate; *P < 0.05, **P < 0.005 and *** P < 0.0005 *vs* control.

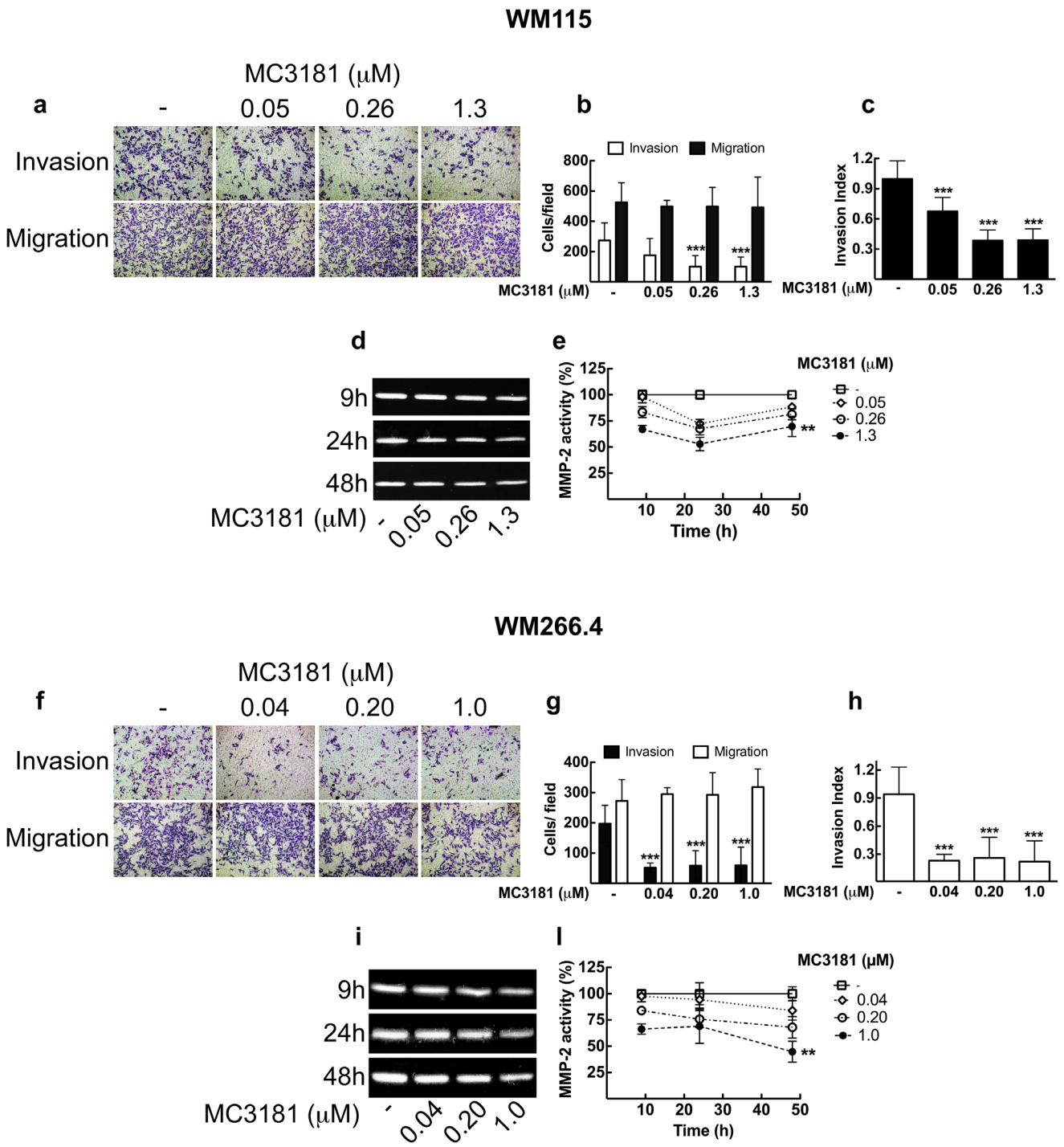

Figure 3: MC3181 blocks WM115 and WM266.4 melanoma cells invasion and inhibits MMP2 activity. Cell lines were assayed for *in vitro* invasion and migration using Boyden chamber without coating (migration) or coated with 5 μg of Matrigel. After 48 hours of treatment with graded MC3181 concentrations, migrated and invaded cells per field were stained with crystal violet and counted. Representative phase contrast images (10X magnification, 3X digital magnification) of **a.** WM115 and **f.** WM266.4 are shown. Migrated/Invaded **b.** WM115 and **g.** WM266.4 cells. The invasion index of **c.** WM115 and **h.** WM266.4 cells was calculated as the invasion percentage of treated cells divided by the invasion percentage of non-treated cells (see equations 2 and 3 in "Materials and Methods" section). Intracellular MMP-2 activity was measured by gelatin zymography assay on **d.** WM115 and **i.** WM266.4 cells treated with graded MC3181 concentrations for up to 48 hours. ImageJ quantification of 3 independent experiments of gelatin zymography performed on **e.** WM115 and **l.** WM266.4 cells. The control has been settled as the 100%, and results were expressed as the mean percentage of MMP-2 activity ± SD *vs* control. **P < 0.005 and ***P < 0.0005 *vs* control.

proteinases 2 and 9 (MMP-2 and MMP-9); the cell-cell adhesion molecules E-cadherin (CDH1), N-cadherin (CDH2), Ve-cadherin (CDH5), and both the long and short isoforms of the endothelial antigen MCAM/MUC18 [11]. To validate our expression panel, we used two melanoma cell lines as positive control (M10 and M14) and β_2-microglobulin as housekeeping.

RT-PCR documented mRNA expression in all the melanoma cell lines analyzed (WM115, WM266.4, and the positive controls M10 and M14) for VEGF, FGF2, CDH2, CDH5, MMP-2, MMP-9, and the two isoforms of MCAM/MUC18. The mRNA expression levels of all the genes tested in WM115 and WM266.4 cell lines are shown in Figure 5a, and a representative gel is reported in Supplementary Figure 5. Afterwards, we analyzed the mRNA expression of these genes following treatment with equiactive concentrations of MC3181 (corresponding to its IC_{50} value, 1/5 and 1/25 of its IC_{50} value in these cell lines). CDH5, VEGF, FGF2, MMP-2, MMP-9 and both the MCAM/MUC 18 Long and Short isoforms mRNA were still present at 24 hours in WM115 cells, while they drastically decreased at 48 hours after treatment with all the MC3181 concentrations tested (Figure 5a, left). Interestingly, 9 hours of drug exposure were sufficient to induce a drastic decrease of the CDH2 mRNA (Figure 5a, left). Conversely, a strong reduction of mRNA expression of all genes could be observed in WM266.4 cells after 48 hours of

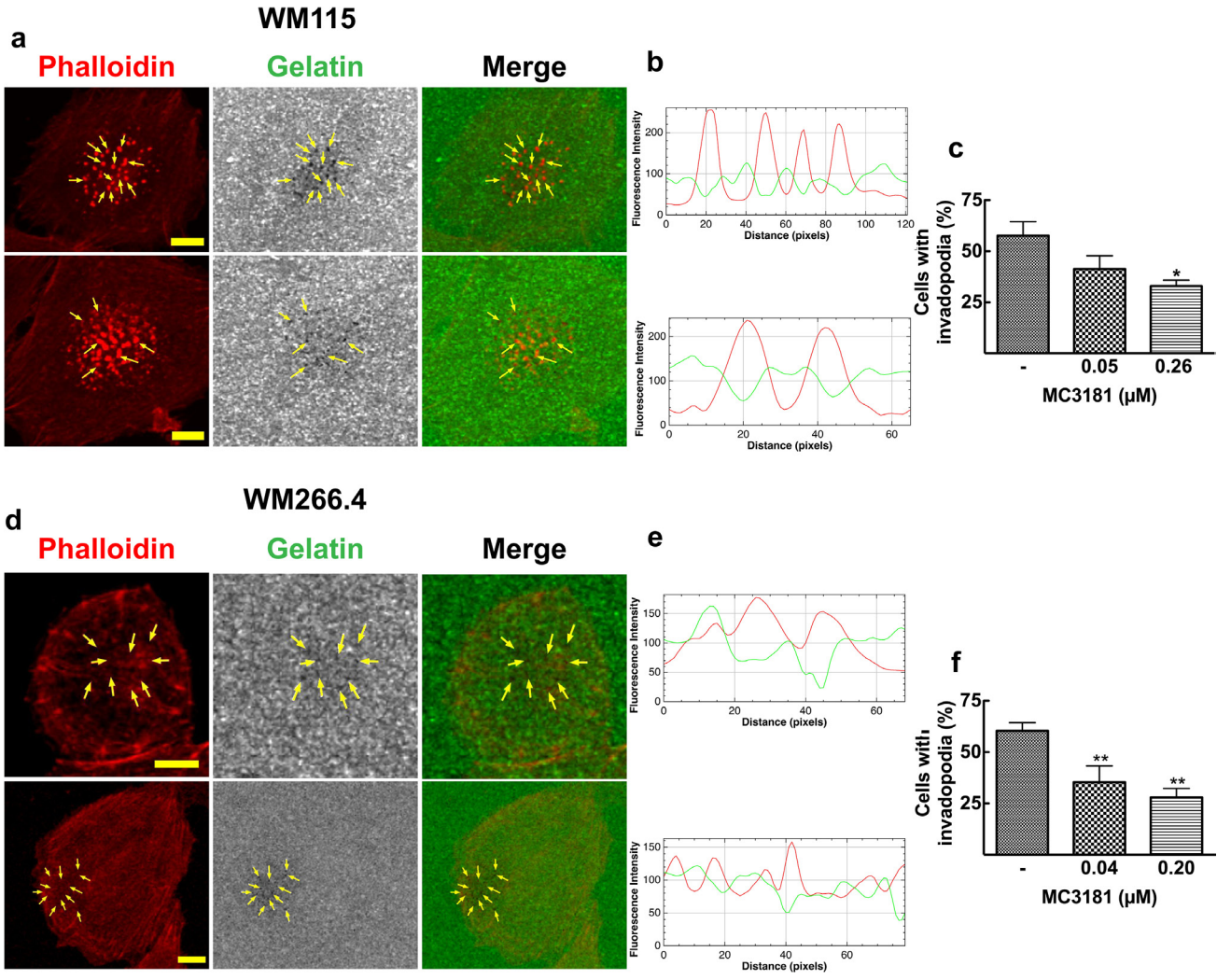

Figure 4: Invadopodia matrix degradation activity. WM115 and WM266.4 cells were seeded on Fluorescein-Gelatin coated chamber slides for 5 hours, and then fixed and stained for TRITC-Phalloidin. **a.** WM115 and **d.** WM266.4 representative confocal images showing invadopodia as focal cytoplasmic concentrations of Phalloidin that overlap with areas of gelatin clearing (dark holes in the matrix) within the merged image, as indicated by arrows. Fluorescein-Gelatin images were pseudocolored in gray. Images were acquired with a 40X magnification oil immersion objective and a digital magnification 3X is shown. Scale bar = 10 μm. **b.** WM115 and **e.** WM266.4 representative fluorescence intensity plot showing co-localization of TRITC-Phalloidin (red line) and gelatin degradation (green line). Fluorescence intensity was measured at each image pixel along an arbitrary line that crossed through an invadopodia structure. Percentage of **c.** WM115 and **f.** WM266.4 cells with active invadopodia was obtained by counting approximately 100 cells in 3 fields. Data shown are means ± SD of three independent experiments. *P < 0.05 and **P < 0.005 *vs* control.

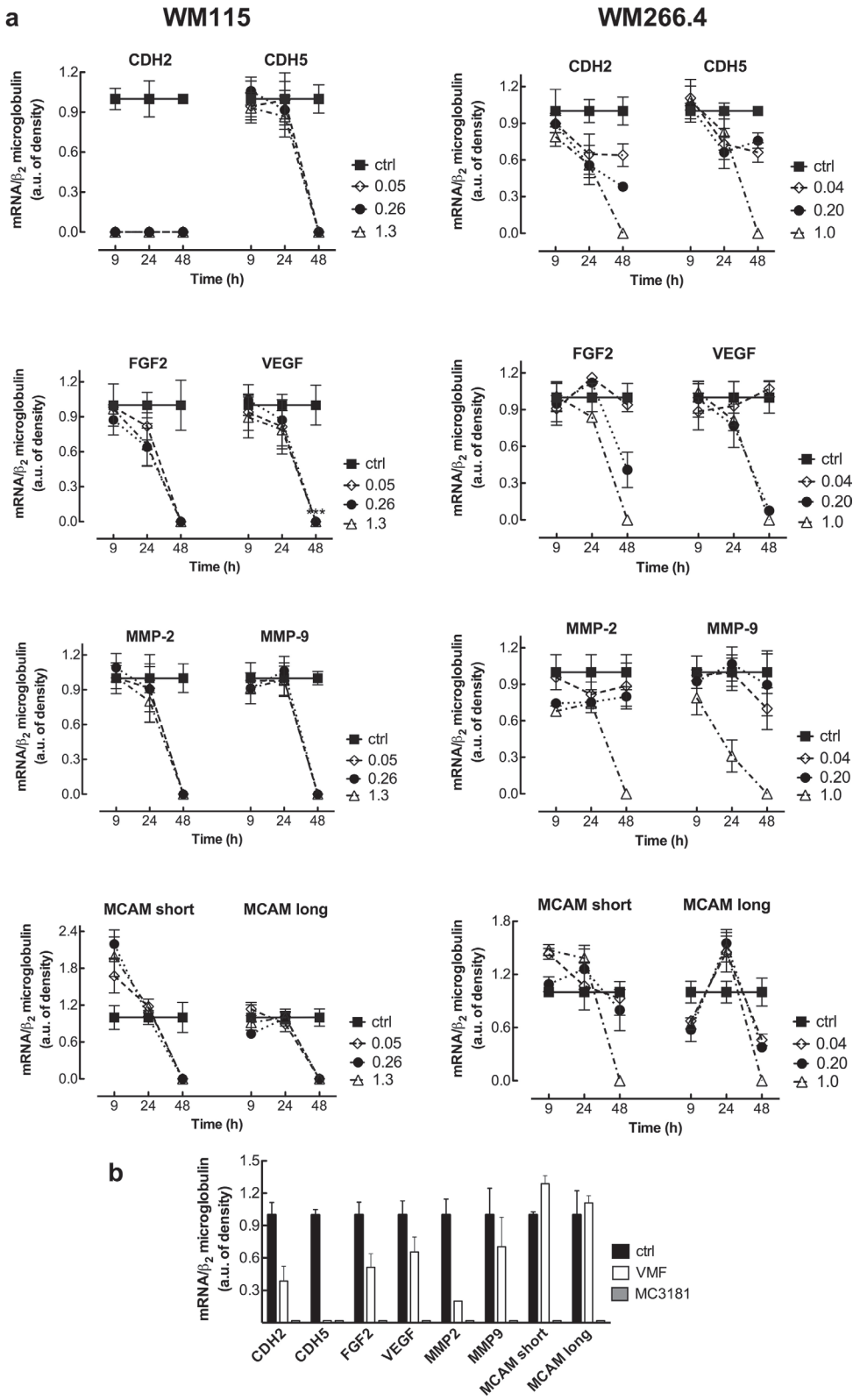

Figure 5: RT-PCR analysis of the mRNA expression of cancer progression related genes. a. Total RNA from untreated and MC3181-treated cells was extracted, reverse-transcribed, amplified by PCR, and submitted to electrophoresis on a 1.8% agarose gel (see "Materials and Methods" section). The graphs show the relative intensity of the PCR products vs β2-microglobulin, obtained by the ImageJ analysis software: -■-ctrl; -◊- 0.05 and 0.04 μM MC3181 (WM115 and WM266.4, respectively); -●- 0.26 and 0.20 μM MC3181 (WM115 and WM266.4, respectively) and -Δ- 1.3 and 1.0 μM MC3181 (WM115 and WM266.4, respectively). **b.** Relative intensity of the PCR products from WM266.4 cells treated for 48 hours with equiactive concentrations of MC3181 and VMF (1.0 μM *vs* 0.9 μM, respectively).

treatment only with the highest concentration (1.0 μM) of MC3181 (Figure 5a, right). We did not detect the presence of CDH1 mRNA in both WM115 and WM266.4 cell lines, either before or after MC3181 treatment (data not shown).

Finally, we decided to perform a preliminary comparison of the efficacy of equiactive concentrations of MC3181 and VMF, corresponding to their IC_{50} values (1.0 and 0.9 μM, respectively), on the mRNA expression. Interestingly, we found that MC3181 treatment outperformed VMF in the suppression of the genes analyzed after 48 hours, with the only exception of CDH5 (Figure 5b).

MC3181 inhibits WM266.4 3D-multicellular tumor spheroid invasion into collagen type I

Tumor invasion was further analyzed in WM115 and WM266.4 cells grown as 3D-multicellular tumor spheroids and embedded in type I collagen. Under these experimental conditions, spheroids formed by WM115 cells were not able to invade the collagen matrix, and therefore subsequent experiments were performed only on WM266.4 cells. Also in this case, the compound was able to significantly reduce cells invasion into collagen, in a dose dependent manner (Figure 6). Twenty-four hour treatment with 0.04, 0.20 and 1.0 μM MC3181 reduced the distance invaded by WM266.4 cells by about 40, 60 and 80%, respectively, compared to the control. The effect obtained with 0.20 and 1.0 μM MC3181 remained constant over the 48 hours incubation period, while spheroids treated with 0.04 μM MC3181 showed a recovery of their invasive potential.

MC3181 down-regulates the phospho-activation of c-Jun N-terminal kinase (JNK) and p38

To gain insight about the molecular mechanisms, we analyzed the effect of MC3181 treatment on proteins involved in WM266.4 cell invasion. Since activation of the MAPK/ERK pathway is a frequent event in tumorigenesis, we investigated the activation level of

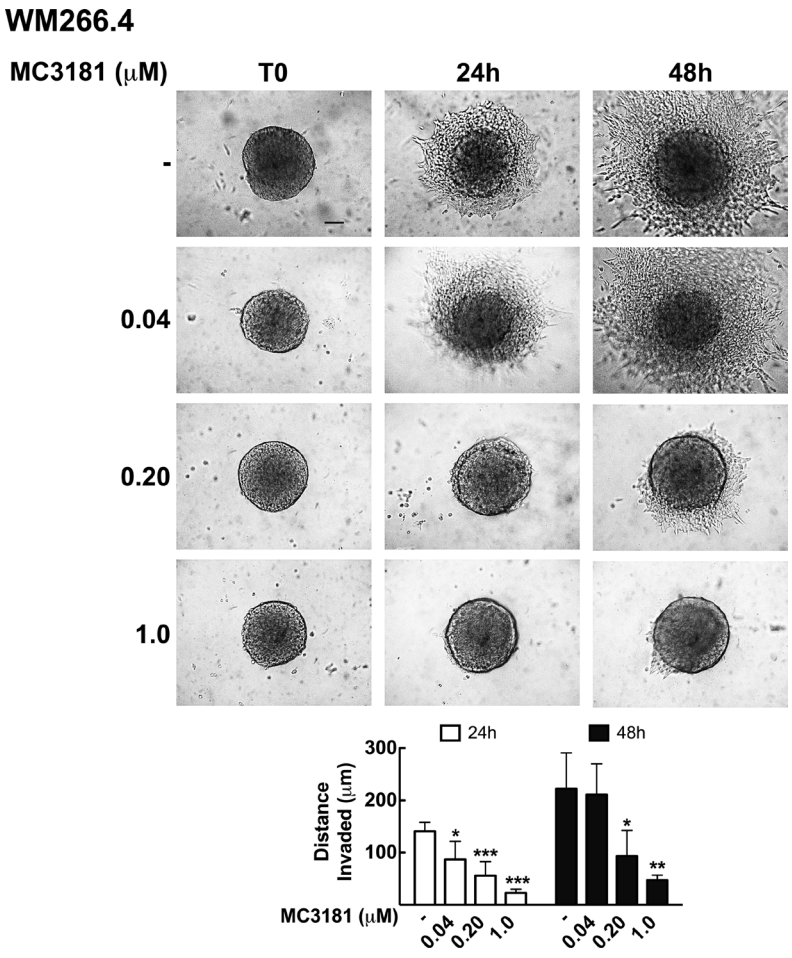

Figure 6: MC3181 inhibits WM266.4 spheroids invasion into type I collagen. 3D melanoma spheroids were embedded in a collagen matrix and treated with 0.04, 0.20 and 1.0 μM MC3181. The distance invaded by WM266.4 cells was monitored by phase contrast imaging (10X magnification, 3X digital magnification), over a 48 hours incubation period. Scale bar: 100 μm. The graph shows the mean distance invaded by spheroids ± SD; sample number: n = 10 for every condition; *P < 0.05, **P < 0.005 and ***P < 0.0005 *vs* the respective time-matched control.